



Cite this: *RSC Adv.*, 2024, 14, 5846

Received 2nd February 2024  
Accepted 8th February 2024

DOI: 10.1039/d4ra00845f

rsc.li/rsc-advances

# Highly electron-deficient 1-propyl-3,5-dinitropyridinium: evaluation of electron-accepting ability and application as an oxidative quencher for metal complexes†

Akitaka Ito, <sup>ID</sup>\*<sup>ab</sup> Yasuyuki Kuroda,<sup>a</sup> Kento Iwai, <sup>ID</sup><sup>ab</sup> Soichi Yokoyama <sup>ID</sup>†<sup>ab</sup>  
and Nagatoshi Nishiwaki <sup>ID</sup>\*<sup>ab</sup>

Impacts of the nitro groups on the electron-accepting and oxidizing abilities of *N*-propylpyridinium were evaluated quantitatively. A 3,5-dinitro derivative has efficiently quenched emission from photosensitizing Ru(II) and Ir(III) complexes owing to the thermodynamically-favored electron transfer to the pyridinium whose LUMO is greatly lowered by the presence of electron-withdrawing nitro groups.

## Introduction

Pyridines are typical electron-deficient heterocyclic compounds that can be seen all around us as substructures of functional materials such as pharmaceuticals, ligands, and optical and electronic devices.<sup>1</sup> The nucleophilic ring nitrogen, furthermore, undergoes *N*-alkylation, resulting in pyridinium salt. Owing to their highly electron-deficient aromatic character, pyridinium skeletons have been utilized in a variety of natural/artificial systems as electron acceptors as represented by NAD<sup>+</sup>,<sup>2</sup> methyl viologen<sup>3</sup> and so forth.<sup>4</sup> On the other hand, a nitro group exhibits strong electron-withdrawing ability due to both resonance and inductive effects, with the latter effect equivalent to two chloro groups.<sup>5</sup> Therefore, a combination of the highly electron-deficient pyridinium and strong electron-withdrawing nitro group is expected to significantly increase the oxidation or electron-accepting abilities.

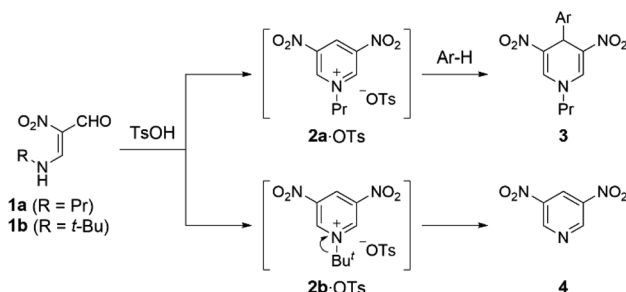
In our previous work, we have demonstrated that 1-propyl-3,5-dinitropyridinium salt **2a**·OTs is formed *in situ* upon treatment of *N*-propyl-β-formyl-β-nitroenamine **1a** (R = Pr) with *p*-toluenesulfonic acid (TsOH), and formation of the salt **2a**·OTs is confirmed by trapping as 4-arylated 1,4-dihydropyridine derivatives **3** with electron-rich benzenes.<sup>6</sup> On the other hand, 3,5-dinitropyridine **4** was obtained when *N*-*tert*-butylenamine

**1b** (R = *t*-Bu) was subjected to the same reaction, which is because a stable *tert*-butyl cation is readily eliminated (Scheme 1). The easy access to 3,5-dinitropyridine **4** facilitates the *N*-modification to afford versatile *N*-alkyl-3,5-dinitropyridinium salts **2**. Indeed, treatment of **4** with propyl triflate (PrOTf) proceeded at room temperature to furnish **2a**·OTf. This easily modifiable feature prompted us to evaluate the electron-acceptability of its *N*-alkylated form (**2a**<sup>+</sup>) by comparing with 3-nitro and unsubstituted pyridinium relatives (**5**<sup>+</sup> and **6**<sup>+</sup>) that are prepared from commercially available pyridines by *N*-propylation.

## Experimental

### Preparation of **2a**·OTf

A mixture of 3,5-dinitropyridine **4** (86 mg, 0.5 mmol) and PrOTf (122 mg, 0.63 mmol) was stirred without solvent at room temperature for 2 d. Colorless precipitates were collected and washed with CH<sub>2</sub>Cl<sub>2</sub> to afford **2a**·OTf (95 mg, 0.28 mmol, 56%) as colorless powder, mp 217.0–217.8 °C. <sup>1</sup>H NMR (400 MHz, CD<sub>3</sub>CN) δ 1.03 (t, *J* = 7.6 Hz, 3H), 2.12 (tq, *J* = 7.6, 7.6 Hz, 2H),



Scheme 1 Generation of 1-alkyl-3,5-dinitropyridinium salts **2**·OTs *in situ* from *N*-alkyl-β-formyl-β-nitroenamines **1**.

<sup>a</sup>School of Engineering Science, Kochi University of Technology, Tosayamada, Kami, Kochi 782-8502, Japan. E-mail: ito.akitaka@kochi-tech.ac.jp, nishiwaki.nagatoshi@kochi-tech.ac.jp

<sup>b</sup>Research Center for Molecular Design, Kochi University of Technology, Tosayamada, Kami, Kochi 782-8502, Japan

† Electronic supplementary information (ESI) available: Cyclic voltammograms of the metal complexes and emission quenching data by **5**<sup>+</sup> and **6**<sup>+</sup>. See DOI: <https://doi.org/10.1039/d4ra00845f>

‡ Present address: The Institute of Scientific and Industrial Research (SANKEN), Osaka University, Ibaraki, Osaka 567-0047, Japan.



4.80 (t,  $J = 7.6$  Hz, 2H), 9.78 (t,  $J = 2.0$  Hz, 1H), 9.94 ppm (d,  $J = 2.0$  Hz, 2H);  $^{13}\text{C}$  NMR (100 MHz,  $\text{CD}_3\text{CN}$ )  $\delta$  10.2 ( $\text{CH}_3$ ), 25.3 ( $\text{CH}_2$ ), 66.5 ( $\text{CH}_2$ ), 121.8 (q,  $J = 318.0$  Hz,  $\text{CF}_3$ ), 135.9 (CH), 147.3 (CH), 147.9 ppm (C);  $^{19}\text{F}$  NMR (376 MHz,  $\text{CD}_3\text{CN}$ )  $\delta$  79.36 ppm; HRMS (ESI-TOF) calcd for  $\text{C}_8\text{H}_{10}\text{N}_3\text{O}_4$  ( $\text{M}^+$ ): 212.0666, found: 212.0676.

### Characterization of 5·OTf

mp 102.3–102.7 °C.  $^1\text{H}$  NMR (400 MHz,  $\text{CD}_3\text{CN}$ )  $\delta$  1.00 (t,  $J = 7.2$  Hz, 3H), 2.06 (tq,  $J = 7.2, 7.2$  Hz, 2H), 4.66 (t,  $J = 7.2$  Hz, 2H), 8.30 (dd,  $J = 8.4$  Hz, 6.2 Hz, 1H), 9.01 (dd,  $J = 6.2, 2.0$  Hz, 1H), 9.18 (ddd,  $J = 8.4, 2.0, 1.2$  Hz, 1H), 9.63 ppm (d,  $J = 1.2$  Hz 1H);  $^{13}\text{C}$  NMR (100 MHz,  $\text{CD}_3\text{CN}$ )  $\delta$  10.3 ( $\text{CH}_3$ ), 25.2 ( $\text{CH}_2$ ), 65.2 ( $\text{CH}_2$ ), 125.1 (q,  $J = 319$  Hz,  $\text{CF}_3$ ), 130.4 (CH), 141.0 (CH), 142.7 (CH), 147.8 (C), 150.1 ppm (CH);  $^{19}\text{F}$  NMR (376 MHz,  $\text{CD}_3\text{CN}$ )  $\delta$  79.31 ppm; HRMS (ESI-TOF) calcd for  $\text{C}_8\text{H}_{11}\text{N}_2\text{O}_2$  ( $\text{M}^+$ ): 167.0815, found: 167.0819.

### Characterization of 6·OTf

$^1\text{H}$  NMR (400 MHz,  $\text{CD}_3\text{CN}$ )  $\delta$  1.00 (t,  $J = 7.6$  Hz, 3H), 2.06 (tq,  $J = 7.6, 7.6$  Hz, 2H), 4.49 (t,  $J = 7.6$  Hz, 2H), 8.03 (br, 2H), 8.51 (t,  $J = 7.6$  Hz, 1H), 8.70 ppm (d,  $J = 5.6$  Hz, 2H);  $^{13}\text{C}$  NMR (100 MHz,  $\text{CD}_3\text{CN}$ )  $\delta$  9.3 ( $\text{CH}_3$ ), 24.0 ( $\text{CH}_2$ ), 62.9 ( $\text{CH}_2$ ), 120.9 (q,  $J = 318$  Hz,  $\text{CF}_3$ ), 128.1 (CH), 144.2 (CH), 145.5 ppm (CH);  $^{19}\text{F}$  NMR (376 MHz,  $\text{CD}_3\text{CN}$ )  $\delta$  79.30 ppm; HRMS (ESI-TOF) calcd for  $\text{C}_8\text{H}_{12}\text{N}$  ( $\text{M}^+$ ): 122.0964, found: 122.0966.

### Other chemicals

$[\text{Ru}(\text{bpy})_3](\text{PF}_6)_2$  (bpy = 2,2'-bipyridine) is the same sample which has been used in the earlier literatures.<sup>7</sup>  $[\text{Ir}(\text{ppy})_2(\text{bpy})]\text{PF}_6$  (ppyH = 2-phenylpyridine) was synthesized and purified similarly to the reported procedure.<sup>8</sup> Tetra-*n*-butylammonium hexafluorophosphate (TBAPF<sub>6</sub>, Wako Pure Chemical Industries) was purified by repeated recrystallizations from ethanol. Ferrocene (Wako Pure Chemical Industries) was used as supplied. Anhydrous or spectroscopic-grade  $\text{CH}_3\text{CN}$  (Wako Pure Chemical Industries) was used without further purification for the electrochemical or spectroscopic measurements, respectively.

### Electrochemical measurements

Cyclic voltammetry of the complexes in  $\text{CH}_3\text{CN}$  at 298 K was performed by using a BAS ALS-1202A electrochemical analyzer with a three-electrode system using glassy-carbon working, Ag auxiliary, and Ag/AgNO<sub>3</sub> reference electrodes ( $\sim 0.01$  mol dm<sup>-3</sup> (=M) in  $\text{CH}_3\text{CN}$  containing  $\sim 0.1$  M TBAPF<sub>6</sub>) supplied by BAS Inc. The sample solutions containing a pyridinium salt or metal complex ( $\sim 1.0$  mM) and TBAPF<sub>6</sub> as a supporting electrolyte ( $\sim 0.1$  M) in the absence or presence of ferrocene as an internal standard were deaerated by purging an argon-gas stream over 20 min prior to measurements. The potential sweep rate was 100 mV s<sup>-1</sup>.

### Emission quenching study

Emission spectra were recorded and emission quantum yields ( $\Phi_{\text{em}}$ ) were determined by the absolute method using

a Hamamatsu Photonics Quantaaurus-QY Plus C13534-02. Emission intensity at each wavelength was corrected for system spectral response so that the vertical axis of a spectrum corresponds to the photon number at each wavelength. Emission decay profiles of  $[\text{Ir}(\text{ppy})_2(\text{bpy})]\text{PF}_6$  was measured by using a Hamamatsu C4334 streak camera with a C5094 polychromator by exciting at 400 nm using second harmonics of a femtosecond-pulse mode-locked Ti:sapphire laser (MKS Instruments Spectra-Physics Tsunami® 3941-M1BB and 3980 frequency doubler/pulse selector, 1 MHz) and analyzed by a single exponential decay function. Sample solutions were deaerated by purging with an argon-gas stream for over 30 min.

Free energy changes for the electron-transfer processes ( $-\Delta G$ ) were calculated by:<sup>9</sup>

$$-\Delta G = nF[E_{1/2}(\text{Q}^{+/0}) - E_{1/2}(\text{M}^*)] + Z_{\text{Q}}Z_{\text{M}}e^2/D_{\text{s}}d = nF[E_{1/2}(\text{Q}^{+/0}) - E_{1/2}(\text{M})] + E_0(\text{M}^*) + Z_{\text{Q}}Z_{\text{M}}e^2/D_{\text{s}}d \quad (1)$$

In eqn (1),  $E_{1/2}(\text{Q}^{+/0})$  is the reduction potential of  $\text{Q}^+$ , and  $E_{1/2}(\text{M})$  is the oxidation potential of the complex (1.32 and 1.63 V vs. SCE for  $[\text{Ru}(\text{bpy})_3]^{2+}$  and  $[\text{Ir}(\text{ppy})_2(\text{bpy})]^+$ , respectively, see Fig. S1†).  $E_0(\text{M}^*)$  is the excited-state zeroth energy and has been determined to be 16 360 and 16 850 cm<sup>-1</sup> for  $[\text{Ru}(\text{bpy})_3]^{2+}$  and  $[\text{Ir}(\text{ppy})_2(\text{bpy})]^+$ , respectively, by the Franck–Condon analysis.<sup>10</sup>  $Z_{\text{Q}}$  and  $Z_{\text{M}}$  are the charges of  $\text{Q}^+$  and complex.  $d$  is the sum of effective radii of  $\text{Q}^+$  and complex estimated for the optimized geometries by DFT calculations (4.7, 4.6, 4.4, 6.2 and 6.2 Å for  $2\text{a}^+$ ,  $5^+$ ,  $6^+$ ,  $[\text{Ru}(\text{bpy})_3]^{2+}$  and  $[\text{Ir}(\text{ppy})_2(\text{bpy})]^+$ , respectively).  $D_{\text{s}}$ ,  $n$ ,  $F$  and  $e$  are the static dielectric constant of the solvent (relative dielectric constant of  $\text{CH}_3\text{CN}$ : 37.5), the number of electrons transferred, the Faraday constant and the formal charge, respectively. It should be noted that, in eqn (1), an electrostatic work term for the electron-transfer products was omitted since the reduced pyridiniums are charge-neutral.

### Theoretical calculations

Theoretical calculations for the compounds were conducted with Gaussian 09W software (Revision C.01).<sup>11</sup> The ground-state geometries of the pyridinium cations were optimized by using density functional theory (DFT) using the restricted B3LYP functional with 6-31+G(d,p) basis set. All the optimized geometries did not gave any negative frequencies under identical methodologies. Lowest-energy unoccupied molecular orbitals were plotted using GaussView 5.<sup>12</sup> All the calculations were carried out as in acetonitrile by using a polarizable continuum model (PCM).

## Results and discussion

Down-field shifts of the ring protons in the  $^1\text{H}$  NMR spectra in  $\text{CD}_3\text{CN}$  were observed as the number of nitro groups increased (Fig. 1), indicating a decrease in the electron density of the pyridine ring. All the pyridiniums  $2\text{a}^+$ ,  $5^+$  and  $6^+$  in  $\text{CH}_3\text{CN}$  exhibited an irreversible reduction wave as shown in Fig. 2. Half reduction potential ( $E_{1/2}$ ) was shifted to a positive potential region with increasing the nitro group ( $E_{1/2} = -0.061$  ( $2\text{a}^+$ ),  $-0.41$  ( $5^+$ ) and  $-0.80$  V ( $6^+$ ) vs. saturated calomel electrode



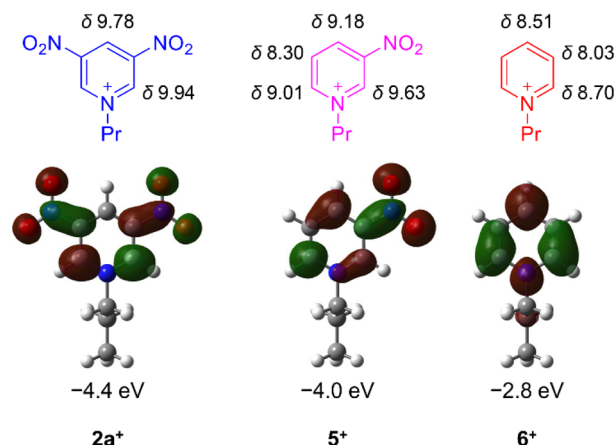


Fig. 1 Chemical shifts of  $^1\text{H}$  NMR in  $\text{CD}_3\text{CN}$  (given in ppm) and LUMO distributions/energies of pyridiniums **2a<sup>+</sup>**, **5<sup>+</sup>** and **6<sup>+</sup>**.

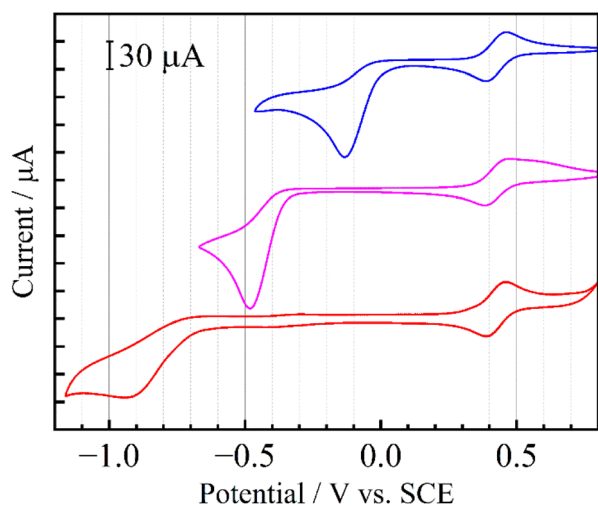


Fig. 2 Cyclic voltammograms of **2a<sup>+</sup>·OTf** (blue), **5<sup>+</sup>·OTf** (pink) and **6<sup>+</sup>·OTf** (red) in deaerated  $\text{CH}_3\text{CN}$  containing 0.1 M TBAPF<sub>6</sub>. Reversible waves at around +0.43 V represent redox couples of ferrocene as an internal standard.

(SCE)). These tendencies were supported by DFT calculations, as the LUMO energy of **2a<sup>+</sup>** was lowered to -4.4 eV (see Fig. 1). It is, furthermore, worth emphasizing that the  $E_{1/2}$  value of **2a<sup>+</sup>** is surprisingly positive even by comparing with that of methyl viologen (-0.44 V vs. sodium saturated calomel electrode (SSCE)<sup>13</sup>). In contrast to fully reversible redox behavior of methyl viologen and resulting applications as a redox shuttle,<sup>3</sup> the highly-positive reduction potential of **2<sup>+</sup>** is advantageously utilizable as a sacrificial electron acceptor in the various photochemical systems.

The strong electron-accepting ability of **2a<sup>+</sup>** is utilizable as an oxidative quencher in photoinduced electron-transfer reactions. As shown in Fig. 3(a), emission from a famous photosensitizer  $[\text{Ru}(\text{bpy})_3]^{2+}$  (ref. 14) in  $\text{CH}_3\text{CN}$  ( $3.8 \times 10^{-5}$  M) was reduced upon addition of **2a<sup>+</sup>** ( $(0.0\text{--}4.0) \times 10^{-3}$  M), and emission quantum yield ( $\Phi_{\text{em}}$ ) of  $[\text{Ru}(\text{bpy})_3]^{2+}$  was decreased from 0.096 to

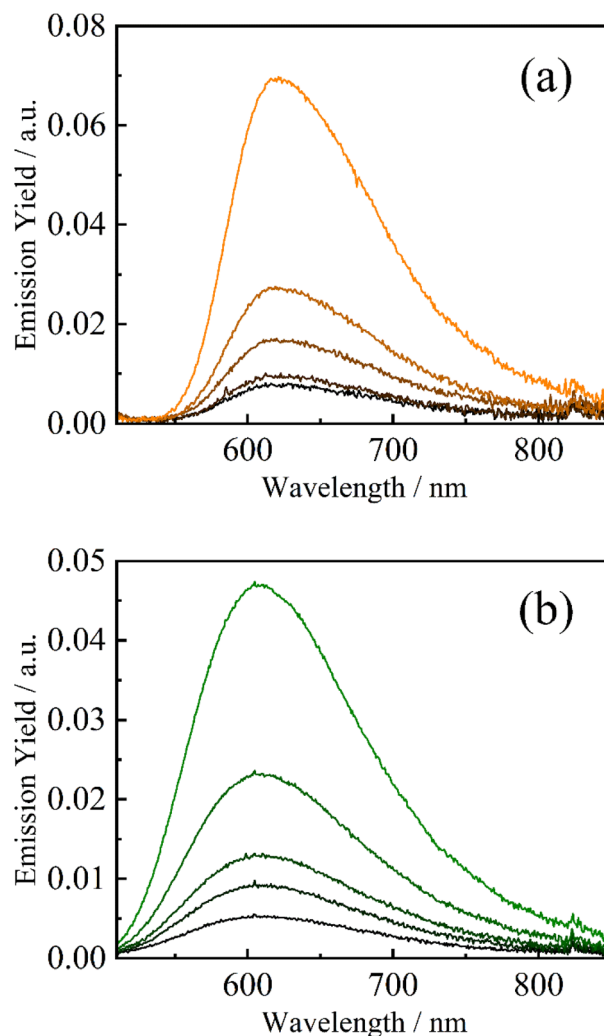


Fig. 3 Emission spectra of  $[\text{Ru}(\text{bpy})_3](\text{PF}_6)_2$  (a,  $3.8 \times 10^{-5}$  M,  $\lambda_{\text{ex}} = 500$  nm) and  $[\text{Ir}(\text{ppy})_2(\text{bpy})]\text{PF}_6$  (b,  $3.8 \times 10^{-4}$  M,  $\lambda_{\text{ex}} = 470$  nm) in the absence and presence of dinitropyridinium salt **2a<sup>+</sup>·OTf** ( $(0.0\text{--}4.0) \times 10^{-3}$  M: orange/green → black) in deaerated  $\text{CH}_3\text{CN}$ .

0.014 in the presence of **2a<sup>+</sup>** ( $4.0 \times 10^{-3}$  M). Emission from a cyclometalated iridium(III) complex  $[\text{Ir}(\text{ppy})_2(\text{bpy})]^+$  in  $\text{CH}_3\text{CN}$  ( $3.8 \times 10^{-4}$  M) was also quenched when **2a<sup>+</sup>** coexisted in a solution ( $\Phi_{\text{em}} = 0.085$  and 0.017 in the absence and presence ( $4.0 \times 10^{-3}$  M) of **2a<sup>+</sup>**, respectively) as shown in Fig. 3(b). Stern-Volmer plots for emission quenching of the complexes by **2a<sup>+</sup>** are shown in Fig. 4, together with those by **5<sup>+</sup>** and **6<sup>+</sup>** (emission spectra are shown in Fig. S2–S5†). The plots exhibited good linear dependences, irrespective of the complex and pyridinium, as expressed by the Stern-Volmer equation:  $\Phi_{\text{em},0}/\Phi_{\text{em}} = 1 + k_q\tau_0[\text{Q}^+]$  with  $\Phi_{\text{em},0}$  and  $\Phi_{\text{em}}$  the emission quantum yields in the absence and presence of the quencher (i.e., **2a<sup>+</sup>**, **5<sup>+</sup>** or **6<sup>+</sup>**), respectively,  $k_q$  the quenching rate constant,  $\tau_0$  the excited-state lifetime of the complex in the absence of the quencher (890 and 300 ns for  $[\text{Ru}(\text{bpy})_3]^{2+}$  and  $[\text{Ir}(\text{ppy})_2(\text{bpy})]^+$ , respectively), and  $[\text{Q}^+]$  the quencher concentration. As clearly seen in Fig. 4 and Table 1, emission quenching by **2a<sup>+</sup>** ( $k_q = 1.6 \times 10^9$  and  $3.2 \times 10^9 \text{ M}^{-1} \text{ s}^{-1}$  for  $[\text{Ru}(\text{bpy})_3]^{2+}$  and  $[\text{Ir}(\text{ppy})_2(\text{bpy})]^+$ , respectively)



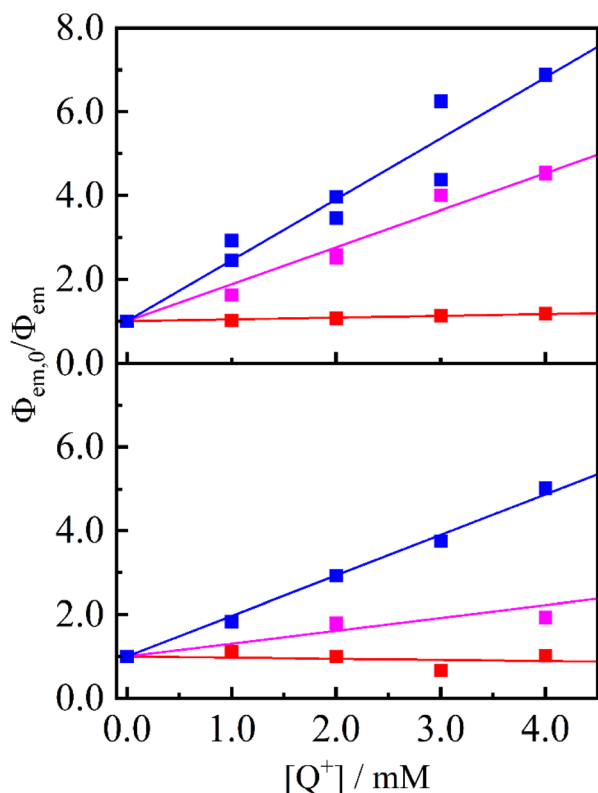


Fig. 4 Stern–Volmer plots for  $[\text{Ru}(\text{bpy})_3]^{2+}$  (top panel) and  $[\text{Ir}(\text{ppy})_2(\text{bpy})]^+$  (bottom panel) quenching by  $2\text{a}^+$  (blue),  $5^+$  (pink) and  $6^+$  (red) in deaerated  $\text{CH}_3\text{CN}$ . Solid lines represent linear regressions with the intercept fixed at 1.

Table 1 Reduction potentials, driving forces for electron transfer and quenching rate constants of pyridiniums  $2\text{a}^+$ ,  $5^+$  and  $6^+$

$\text{Q}^+$	$E_{1/2}/\text{V}$	$[\text{Ru}(\text{bpy})_3]^{2+}$		$[\text{Ir}(\text{ppy})_2(\text{bpy})]^+$	
		$-\Delta G/\text{eV}$	$k_q/10^9 \text{ M}^{-1} \text{ s}^{-1}$	$-\Delta G/\text{eV}$	$k_q/10^9 \text{ M}^{-1} \text{ s}^{-1}$
$2\text{a}^+$	−0.061	+0.72	1.6	+0.43	3.2
$5^+$	−0.41	+0.37	0.99	+0.084	1.0
$6^+$	−0.80	+0.016	0.048	−0.30	<0.01

was more efficient than those by  $5^+$  and  $6^+$  ( $k_q \leq 1.0 \times 10^9 \text{ M}^{-1} \text{ s}^{-1}$ ), indicating that the more nitro group, the stronger the quenching ability.

The efficient emission quenching by  $2\text{a}^+$  can be discussed in terms of a driving force of the electron-transfer process ( $-\Delta G$ , Table 1), which is calculated from the reduction potentials of the pyridinium, the oxidation potentials of the excited-state complexes and so forth. The  $k_q$  value correlates well with the  $-\Delta G$  value, suggesting that the observed emission quenching originates in the electron transfer from the metal complex (*i.e.*,  $[\text{Ru}(\text{bpy})_3]^{2+}$  or  $[\text{Ir}(\text{ppy})_2(\text{bpy})]^+$ ) in the excited state to pyridinium (*i.e.*,  $2\text{a}^+$ ,  $5^+$  or  $6^+$ ). It is worth noting that the electron transfer between  $[\text{Ir}(\text{ppy})_2(\text{bpy})]^+$  to  $6^+$  is highly an endergonic process ( $-\Delta G = -0.30 \text{ eV}$ ) and, therefore, no emission quenching has been observed. Thus, an introduction of a nitro

group(s) into a pyridinium skeleton improves the electron-accepting ability.

## Conclusions

A combination of an electron-deficient pyridinium and electron-withdrawing nitro group(s) enhanced electron-accepting and oxidizing abilities. Each nitro-group introduction lowered the LUMO by several tenths of an electron volt, and dinitropyridinium  $2\text{a}^+$  especially served as an excellent oxidative quencher in photoinduced electron-transfer reactions. Since pyridinium derivatives have attracted increasing interest and utilized in a variety of photochemical systems such as natural/artificial photosynthesis, these nitropyridiniums are possible candidates as a new class of electron acceptors.

## Author contributions

A. Ito: conceptualization, data curation, writing – original draft, and supervision. Y. Kuroda, K. Iwai and S. Yokoyama: investigation. N. Nishiwaki: supervision and writing – review & editing.

## Conflicts of interest

There are no conflicts to declare.

## Notes and references

- J. A. Joule and K. Mills, *Heterocyclic Chemistry*, Wiley-Blackwell, New York, 5th edn, 2010.
- A. Fulton and L. E. Lyons, *Aust. J. Chem.*, 1967, **20**, 2267; G. Unden and J. Bongaerts, *Biochim. Biophys. Acta*, 1997, **1320**, 217; J. Barber, *Chem. Phys. Rev.*, 2009, **38**, 185.
- K. Kalyanasundaram, J. Kiwi and M. Grätzel, *Helv. Chim. Acta*, 1978, **61**, 2720; H. Misawa, H. Sakuragi, Y. Usui and K. Tokumaru, *Chem. Lett.*, 1983, **12**, 1021; A. Bose, P. He, C. Liu, B. D. Ellman, R. J. Twieg and S. D. Huang, *J. Am. Chem. Soc.*, 2002, **124**, 4; A. Ito, D. J. Stewart, Z. Fang, M. K. Brennaman and T. J. Meyer, *Proc. Natl. Acad. Sci. U.S.A.*, 2012, **109**, 15132; H. Yamamoto, M. Taomoto, A. Ito and D. Kosumi, *J. Photochem. Photobiol., A*, 2020, **401**, 112771.
- D. Mauzerall and F. H. Westheimer, *J. Am. Chem. Soc.*, 1955, **77**, 2261; S. Fukuzumi, S. Koumitsu, K. Hironaka and T. Tanaka, *J. Am. Chem. Soc.*, 1987, **109**, 305; A. Kobayashi, H. Konno, K. Sakamoto, A. Sekine, Y. Ohashi, M. Iida and O. Ishitani, *Chem.-Eur. J.*, 2005, **11**, 4219; S. Ikeyama and Y. Amao, *ChemCatChem*, 2017, **9**, 833.
- N. Nishiwaki and M. Ariga, *Top. Heterocycl. Chem.*, 2007, **8**, 43.
- H. Asahara, M. Hamada, Y. Nakaike and N. Nishiwaki, *RSC Adv.*, 2015, **5**, 90778; Y. Nakaike, N. Nishiwaki, M. Ariga and Y. Tobe, *J. Org. Chem.*, 2014, **79**, 2163.
- A. Ito, D. J. Stewart, Z. Fang, M. K. Brennaman and T. J. Meyer, *Proc. Natl. Acad. Sci. USA*, 2012, **109**, 15132; A. Ito, D. J. Stewart, T. E. Knight, Z. Fang,

- M. K. Brennaman and T. J. Meyer, *J. Phys. Chem. B*, 2013, **117**, 3428; A. Ito, Z. Fang, M. K. Brennaman and T. J. Meyer, *Phys. Chem. Chem. Phys.*, 2014, **16**, 4880.
- 8 J. Sun, F. Zhong, X. Yi and J. Zhao, *Inorg. Chem.*, 2013, **52**, 6299.
- 9 Gibbs energy of photoinduced electron transfer, in *IUPAC Compendium of Chemical Terminology*, International Union of Pure and Applied Chemistry (IUPAC), 3rd edn, 2019, DOI: [10.1351/goldbook.GT07388](https://doi.org/10.1351/goldbook.GT07388).
- 10 A. Ito and T. J. Meyer, *Phys. Chem. Chem. Phys.*, 2012, **14**, 13731.
- 11 M. J. Frisch, G. W. Trucks, H. B. Schlegel, G. E. Scuseria, M. A. Robb, J. R. Cheeseman, G. Scalmani, V. Barone, B. Mennucci, G. A. Petersson, H. Nakatsuji, M. Caricato, X. Li, H. P. Hratchian, A. F. Izmaylov, J. Bloino, G. Zheng, J. L. Sonnenberg, M. Hada, M. Ehara, K. Toyota, R. Fukuda, J. Hasegawa, M. Ishida, T. Nakajima, Y. Honda, O. Kitao, H. Nakai, T. Vreven, J. J. A. Montgomery, J. E. Peralta, F. Ogliaro, M. Bearpark, J. J. Heyd, E. Brothers, K. N. Kudin, V. N. Staroverov, R. Kobayashi, J. Normand, K. Raghavachari, A. Rendell, J. C. Burant, S. S. Iyengar, J. Tomasi, M. Cossi, N. Rega, J. M. Millam, M. Klene, J. E. Knox, J. B. Cross, V. Bakken, C. Adamo, J. Jaramillo, R. Gomperts, R. E. Stratmann, O. Yazyev, A. J. Austin, R. Cammi, C. Pomelli, J. W. Ochterski, R. L. Martin, K. Morokuma, V. G. Zakrzewski, G. A. Voth, P. Salvador, J. J. Dannenberg, S. Dapprich, A. D. Daniels, O. Farkas, J. B. Foresman, J. V. Ortiz, J. Cioslowski and D. J. Fox, *Gaussian 09 (Revision C.01)*, Gaussian, Inc., Wallingford, CT, 2009.
- 12 R. Dennington, T. Keith and J. Millam, *GaussView Version 5*, Semichem Inc., Shawnee Mission, KS, 2009.
- 13 J. N. Younathan, W. E. Jones and T. J. Meyer, *J. Phys. Chem.*, 1991, **95**, 488.
- 14 D. W. Thompson, A. Ito and T. J. Meyer, *Pure Appl. Chem.*, 2013, **85**, 1257.
- 15 A. Nakagawa, E. Sakuda, A. Ito and N. Kitamura, *Inorg. Chem.*, 2015, **54**, 10287.

